International Journal of Greenhouse Gas Control 153 (2026) 104656

Contents lists available at ScienceDirect

International Journal of Greenhouse Gas Control

journal homepage: www.elsevier.com/locate/ijggc

Operation experience in a Calcium Looping plant using biomass as a fuel in a 2MW$_{th}$ oxy-fired circulating fluidized bed calciner

Borja Arias [a,*], Alberto Méndez [a], Yolanda Álvarez Criado [a], Paula Marqués [a], Roberto García [a], Javier Camús [a], Igor Finca [b], Martin Haaf [c], J.Carlos Abanades [a]

[a] CSIC-INCAR, Francisco Pintado Fe, 26, Oviedo 33011, Spain
[b] HUNOSA, Avenida de Galicia 44 33005 Oviedo, Spain
[c] Sumitomo SHI FW Energia Oy, Metsänneidonkuja 10 02130 Espoo, Finland

ARTICLE INFO

Keywords:
CO_2 capture
Calcium looping
Oxy-fuel calcination
Biomass combustion

ABSTRACT

This study presents recent experimental results from the 1.7 MW$_{th}$ "La Pereda" Calcium Looping pilot plant, following its upgrade to enable biomass combustion in the oxy-fired circulating fluidized bed combustor-calciner which is the main focus of this work. New steady-state trials were conducted under oxy-combustion conditions using biomass pellets in the calciner, accumulating >1500 h of additional experience. A key objective of the new experiments was to leverage the high reactivity of biomass as a fuel to enable combustion under conditions of low oxygen excess. This approach resulted in outlet oxygen concentrations in the CO_2-rich flue gas from the calciner close to zero, and nitrogen oxide (NO_x) levels below 20 ppmv. These conditions have the potential to reduce the purification requirements downstream of the CO_2 capture system, while at the same time, the presence of unburnt fuel constituents and/or intermediate combustion products, such as CO and $C_xH_yO_z$, needs to be managed according to the configuration and boundary conditions of the entire CCS/U system. In particular, operation under sub-stoichiometric conditions ($\lambda < 1$) may lead to CO and unburnt hydrocarbon levels that could be incompatible with CO_2 transport for permanent storage. No adverse impacts of biomass firing were observed on sorbent performance or CO_2 capture efficiency, which reached up to 95% under standard conditions.

1. Introduction

Calcium Looping (CaL) is a CO_2 capture technology that uses calcium oxide (CaO) as a sorbent to absorb CO_2 in a carbonator reactor operating at approximately 650 °C, forming calcium carbonate ($CaCO_3$). In a subsequent high-temperature calcination stage usually involving the oxy-combustion of a fuel, the $CaCO_3$ is decomposed at around 900 °C, releasing a concentrated stream of CO_2 and regenerating CaO for reuse in the carbonator. Calcium looping is also referred to as carbonate looping in the literature.

In CaL systems employing Circulating Fluidized Beds (CFB-CaL, shown in Fig. 1, left), the CaO particles continuously cycle through the carbonator and calciner. The intense solid circulation between carbonator and calciner typical of CFBs allows for steady operation, even with modest CaO to $CaCO_3$ molar conversion ratios (typically around 0.05–0.1). One major advantage of CFB-CaL systems is their ability to efficiently recover the heat required for the endothermic decomposition of $CaCO_3$. This heat can be reclaimed at boiler-level temperatures within the carbonator or elsewhere in the system, minimizing the overall energy penalty (Hanak et al., 2015; Martínez et al., 2016; Perejón et al., 2016; Shimizu et al., 1999; Ströhle et al., 2009). In a recent review of CaL pilot projects, Tan et al. (Tan et al.,. 2024) summarizes the characteristics and operational status of facilities ranging from 1 kW$_{th}$ to large-scale pilots demonstrating performance at the MW$_{th}$ level (Alonso et al., 2014; Arias et al., 2018; Chang et al., 2013; Diego and Alonso, 2016; Dieter et al., 2013; Ströhle et al., 2014). Most large-scale pilots use two interconnected Circulating Fluidized Bed reactors (Fig. 1, left). These systems benefit from structural and operational similarities to Circulating Fluidized Bed Combustion (CFBC) boilers, including comparable materials, solid circulation behavior, gas flow dynamics, and combustion environments. These similarities also facilitate safe interconnection between reactors (Abanades et al., 2009; Arias et al., 2018; Arias et al., 2013; Dieter et al., 2013; Hilz et al., 2017).

Another benefit of CaL systems is the potential use of opportunity fuels in the oxy-fired CFB calciner. The use of biomass and solid SRF has been tested as fuel in the 1 MWt pilot plant in Darmstadt (Haaf et al.,

* Corresponding author at: Carbon Science and Technology Institute, Oviedo, Asturias Spain.
E-mail address: borja@incar.csic.es (B. Arias).

https://doi.org/10.1016/j.ijggc.2026.104656
Received 30 May 2025; Received in revised form 12 March 2026; Accepted 3 April 2026
Available online 8 April 2026

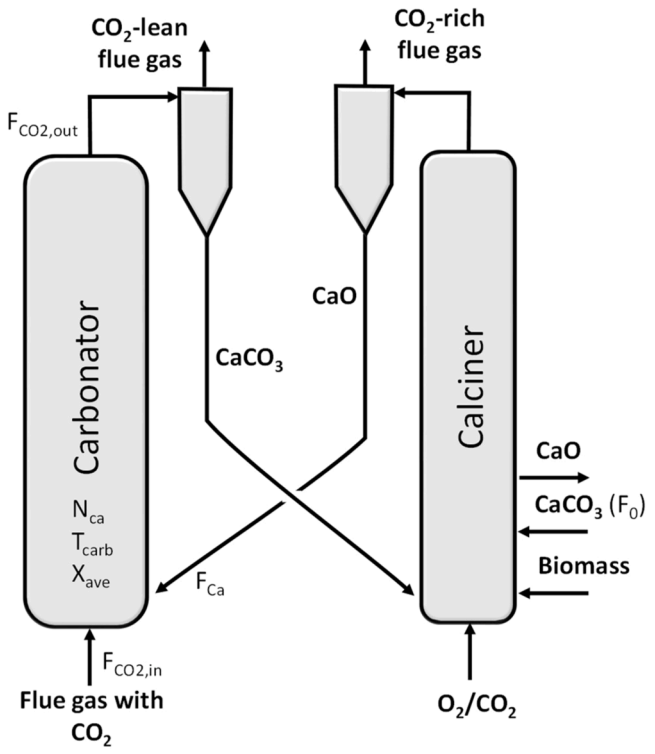

Fig. 1. Left) Scheme of a CFB-CaL system retrofitted to biomass firing in the calciner.

2020; Haaf et al., 2020) and in the 200 kWth pilot plant in Stuttgart (Moreno et al., 2021). Results from these pilots confirm both the feasibility of using such fuels and the additional benefit of capturing acid gases (i.e. SO_2 and HCl) in the calciner.

Among the calcium looping pilots, the 1.7 MW_{th} pilot at La Pereda had previously accumulated over 5000 h of operation (Arias et al., 2018; Arias et al., 2013; Diego and Arias, 2020; Diego et al., 2014) under Technology Readiness Level 6–7 conditions (depending on the target application). This included processing up to 1% of the flue gas from the adjacent coal power plant and firing coal in the pilot's calciner (TRL7). As part of the recent Horizon Europe R&D project (CaLby2030) (Calby2030, 2022), the La Pereda CFB-CaL pilot plant (Fig. 1, right) has undergone several retrofits to demonstrate at TRL6 advanced features of CFB-CaL systems when applied to waste-to-energy plants or biomass-fired power plants. These retrofits include modifications to enable testing with wood pellets in the calciner under oxy-combustion conditions, as well as upgrades to the gas analysis system for improved monitoring of gas impurities characteristic of the flue gas source targeted for CO_2 capture and the raw CO_2-rich gas emitted from the oxy-fired calciner.

The presence of gas impurities in the CO_2 raw stream from the capture system is a critical factor in determining the optimal design and cost of the purification equipment needed to protect the downstream CO_2 transport and storage infrastructure (IEAGHG, 2016; Porter et al., 2015; Sonke et al.,. 2022). This is especially important in oxy-combustion-based systems, where 3–6% vol of O_2 is typically present due to an excess of oxygen beyond the stoichiometric requirement to achieve high combustion efficiency. Additionally, acid gases such as NO_x and SO_x—common byproducts of combustion—can further complicate the purification process (IEAGHG, 2016; Koohestanian and Shahraki,. 2021; Magli et al. 2022; Okeke et al., 2023; Porter et al., 2015; Sala et al., 2024) and demand monitoring in the CFB-CaL reactors, in particular in the calciner. Furthermore, reducing the excess of oxygen during biomass combustion would reduce the demand of oxygen in the calciner, thus reducing the energy penalty associated to the air separation unit.

The aim of this work is to present recent operational experience from the La Pereda CFB-CaL pilot plant during biomass firing in the calciner, acquired during a recent project (Calby2030) (Calby2030, 2022). The main novelty of this work is the operation of the calciner under conditions that minimize the O_2 content in the CO_2-rich stream from the calciner, so as to minimize downstream purification efforts. Oxy-combustion with low excess of oxygen, while maintaining the high CO_2 capture efficiencies inherent to CFB-CaL systems, can be particularly relevant given the growing interest in renewable fuels for power generation. Such systems can become carbon-negative when the captured CO_2 is permanently stored, or produce carbon-neutral fuels when the CO_2 is utilized as a precursor (IPCC, 2005).

2. Experimental

Fig. 2 shows a top-view schematic of the main components of the La Pereda 1.7 MW_{th} pilot plant (photograph of Fig. 1 right), along with their location in relation to the main power plant. The pilot can process a 1% slipstream of the flue gas produced by the existing CFB 50 MW_e power plant of "La Pereda". Such power plant has been operated since 1994 with coal as a fuel and is currently undergoing a major retrofit to become a biomass and SRF fired power plant by 2027. The core of the pilot plant consists of two circulating fluidized bed reactors—a carbonator and a calciner—standing 15 m tall, with internal diameters of 0.65 m and 0.75 m, respectively. These reactors are connected through two loop seals as shown in the top view of the pilot of Fig. 2. Temperature control in the carbonator is achieved using bayonet tubes positioned in the upper section of the reactor, that can be adjusted vertically to modify the heat extraction surface area. A more detailed description of this facility can be found elsewhere (Arias et al., 2013; Diego et al., 2016).

In the new experimental campaigns, the pilot has been operated with biomass firing in the calciner but under conditions relatively standard for CFB boilers and/or CFB-CaL systems: gas velocities within the reactors typically range from 2 to 6 m/s, average carbonator temperature from 530 to 660 °C, average calciner temperature from 840 to 945 °C, inventory of solids in the carbonator and calciner from 50 to 900 kg/m^2.

As shown in Fig. 2, the flue gas from the power plant that is the target for CO_2 capture in the CFB-carbonator, is usually taken before the stack using a fan. Due to the prolonged shutdown periods of the main power plant, most of the experiments reported in this work correspond to testing campaigns during which the gases supplied to the carbonator consisted of a synthetic mixture of air and CO_2 delivered from cryogenic tanks. This is why the scale of the testing reported in this work could be qualified as TRL6 instead of the TRL7 used in previous works with the same pilot. To operate the pilot under these conditions, a negative pressure is compulsory (in order to ensure safe exhausting of the gases to the stack) in the return point of the flue gases from the pilot plant to the power plant. Under normal conditions, this is created by the balance between the forced and induced fans of the main power plant. During most of the tests reported in work, the negative pressure was achieved by operating the induced fan of the main power plant. This also allowed to create a flow of air through the main power plant when switched off, avoiding the accumulation of flue gases from the pilot in the body of the main plant (air preheater, electrostatic precipitator and stack).

The composition of gases entering and exiting the carbonator and calciner reactors is continuously monitored using four gas analysers (three standards for combustion gases and a FTIR analysis system to track gas impurities, including NO, NO_2, N_2O, HCl, HF, SO_2, CH_4, CO, C_xH_yO) that can switch their gas sampling to the different ports in the pilot. Gas concentrations in the Results and Discussion section are expressed in dry basis. The solids circulating within the system are periodically analysed by collecting samples from designated ports throughout the facility (between 2 and 10 samples per hour) and then submitted for chemical analysis (carbon, sulphur and ashes) or more detailed kinetic characterisations (TGA for reactivity test or more in-

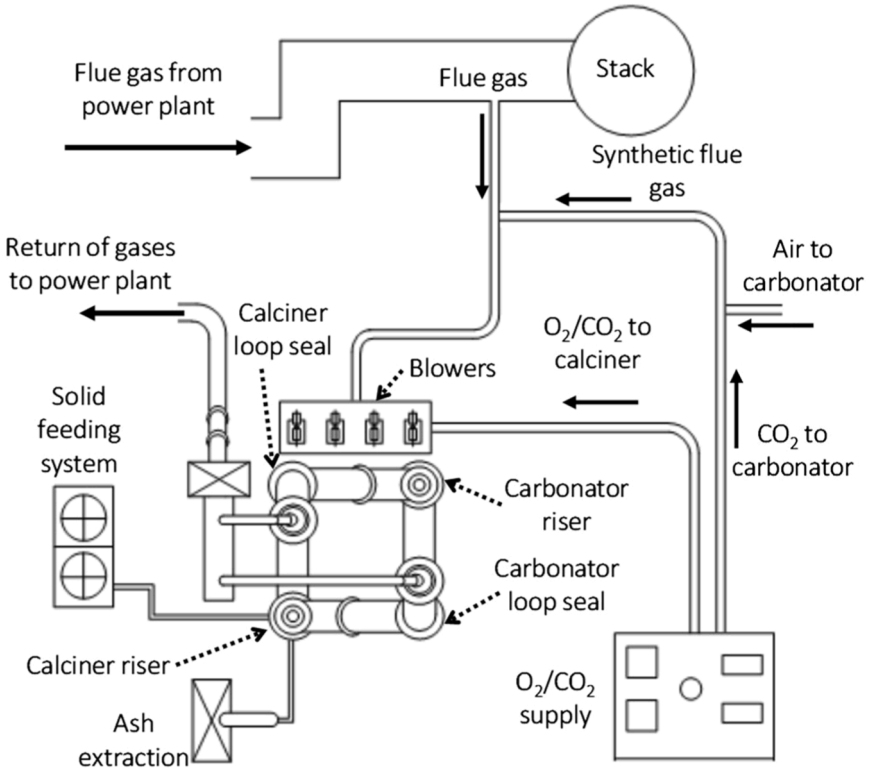

Fig. 2. Top-view scheme of the pilot plant and its integration with the power plant.

depth textural characterisations). The solid circulation between reactors can be monitored during steady states by solving the heat balance in certain control volumes of the pilot (in particular in the loop seals) as discussed in more detail in reference (Arias et al., 2013).

During the experimental campaigns reported in this work, pellets from woody biomass were used as fuel to the calciner (elemental analysis: 50.7%$_{w\ db}$ carbon, 6.0%$_{w\ db}$ hydrogen, 34.6%$_{w\ db}$ oxygen, 0.01%$_{w\ db}$ nitrogen and 0.02%$_{w\ db}$; ultimate analysis: 6.4%$_{w\ ar}$ moisture, 0.5%$_{w}$

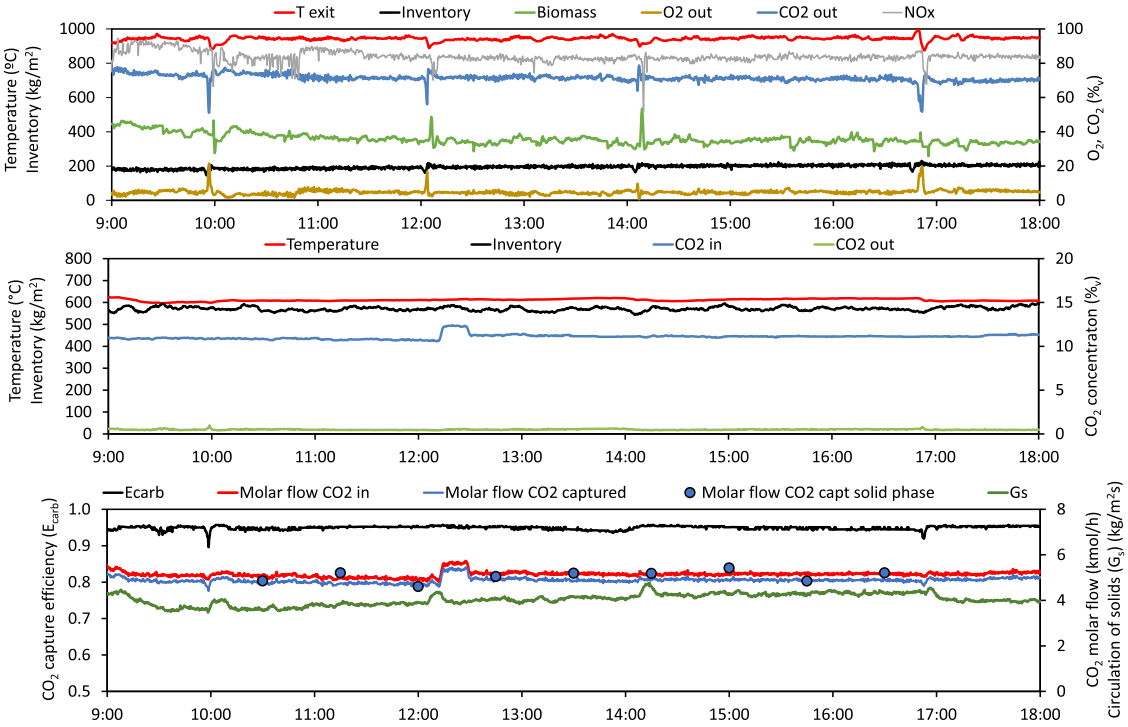

Fig. 3. Example of an experimental CO_2 capture test with oxy-fuel combustion of biomass in the calciner. Top graph: main operation conditions in the calciner; middle graph: main operation conditions in the carbonator; bottom graph: CO_2 capture efficiency (E_{carb}) and molar CO_2 flow entering and captured in the carbonator, circulation of solids (G_s). Average CO_2 carrying capacity of the solids (X_{ave})=0.16.

$_{ar}$ ash, 78.8%$_{w\ ar}$ volatile matter, 14.3%$_{w\ ar}$ fixed carbon; lower heating value (LHV) of 19.1 MJ/kg

3. Results and discussion

After some initial dynamic testing to adjust the new operation protocols, several steady-state trials were conducted to assess the operational performance of the pilot plant using biomass as the fuel in the oxy-fired calciner, as shown in the example of Fig. 3. These tests typically last from 8 to 14 h, with the pilot operating under constant conditions. Initial start-up periods to preheat the pilot and to switch the conditions from air to oxy-fuel conditions in the calciner and from air to flue gas with CO_2 in the carbonator are not shown in this figure. The main operation conditions in the calciner are shown in the top graph of Fig. 3. During this test, the average temperature in the calciner was 940 °C, achieved by burning a biomass flow of 355 kg/h (resulting in a thermal input of 1.88 MW_{th}) using a O_2/CO_2 oxidant mixture with an oxygen concentration of 37%$_v$. The oxygen concentration at the outlet of the calciner was around 4.8%$_v$. With this excess of oxygen, no CO or other unburnt carbon were detected at the outlet of the calciner (not shown in the top graph for simplicity), while an average emission of around 120 ppm$_v$ of NO_x was measured. During this period, the inventory in the calciner was around 200 kg/m^2, which was estimated by the pressure measurements along the reactor. The main operation conditions in the carbonator are shown in the middle graph of Fig. 3. This reactor operated at an average temperature of 610 °C and an inventory of solids of 570 kg/m^2 (see Fig. 3 middle). A flue synthetic flue gas with a CO_2 concentration of 11%$_v$ was fed to the carbonator (which results into an inlet CO_2 molar flow of 5.1 kmol/h).

The total circulation of solids between reactors (in kg/s), can be estimated in this experiment with the closure of the heat balance in the carbonator, because the refractory lining of the pilot unit ensures that heat losses remain limited and can be calibrated with reasonable accuracy. As a result, during steady-state operation, the total solid circulation rate (G_s) entering and exiting the carbonator can be determined by monitoring all relevant parameters in the energy balance—such as temperatures, gas flow rates, and the heat released from the carbonation reaction by the difference in inlet-outlet content of CO_2 in the flue gas—. These measurements can also be calibrated to correct for any systematic discrepancies and provide a similar value (about 4.0 kg/m^{2}s) to that obtained from a similar heat balance in a loop seal (Arias et al., 2018). This method based on heat balances is also routinely validated by comparing with measurements obtained using isokinetic probes. Under the conditions of Fig. 3, the CO_2 concentration achieved at the outlet of the carbonator was 0.5%$_v$ which results into an average capture efficiency (E_{carb}) of 0.95, which is defined as follows:

$$E_{Carb} = \frac{F_{CO2,in} - F_{CO2,out}}{F_{CO2,in}} \quad (1)$$

where $F_{CO2,in}$ and $F_{CO2,out}$ are the molar flows of CO_2 entering and leaving the carbonator.

Several models have been proposed in the literature to analyze the dependencies of CO_2 capture efficiencies in the carbonator with variables such as, temperature, CO_2 inlet concentration in the flue gas, solid inventories, solid circulation rates and average carrying capacity of the sorbent (which depends in turn on sorbent characteristics, make up flows and the calcination conditions in the calciner) during steady-state periods (Greco-Coppi et al., 2025; Lasheras et al., 2011; Romano, 2012; Ylatalo et al., 2012). In this work, a basic model methodology outlined in references (Arias et al., 2013; Charitos et al., 2011) is used to interpret the experimental results obtained during these tests.

To further facilitate comparisons between experiments conducted at different temperatures, it is useful to normalize E_{carb} relative to the maximum CO_2 capture efficiency allowed by the equilibrium ($E_{carb,eq}$), which depends on the average carbonator temperature and its effect on the equilibrium partial pressure of CO_2 (ν_{CO2}). Several equations have been reported in the literature to describe the dependence of the equilibrium CO_2 partial pressure on temperature within the range relevant for CaL systems (Baker, 1962; García-Labiano et al., 2002; Hills, 1968). In this work, the correlation proposed by Baker has been adopted (Baker, 1962).

$$\nu_{CO2,eq} = \frac{10^{(7.079-8308/T)}}{P_{total}} \quad (2)$$

where T is the carbonation temperature (K) and P the total operating pressure (atm).

The molar flow of CO_2 captured in the carbonator ($F_{CO_2,in} - F_{CO_2,out}$) can be experimentally measured using two complementary methods. The first is a carbon mass balance, which requires quantifying the CO_2 removed from the gas phase by monitoring the gas flows entering the carbonator and analysing the flue gas composition before and after the reactor. The second method involves a mass balance on the solid flows circulating between reactors, by determining the molar flow of $CaCO_3$ formed based on changes in the carbonate content of solids entering and exiting the carbonator. Both approaches rely on data from gas analysers, solid circulation rates, and chemical analyses of solid samples. The comparison of the results obtained from both methods is used to validate the consistency of the experimental data. An example of the comparison between both methods is shown in Fig. 3 (bottom), where good agreement is observed, with a value of $F_{CO2,in}$-$F_{CO2,out}$ of approximately 4.9 kmol/h (solid line: CO_2 removal from the gas phase; dots: $CaCO_3$ formed in circulating solids).

On the other hand, the flow of CO_2 disappearing from the gas phase and appearing in the solid circulation phase, must be equal to the CO_2 reacted with the solids present in the carbonator (solid inventory) at any given point in time. Such solids in the carbonator are assumed to react at a rate that follows the simplified reaction rate model (Alonso et al., 2009).

$$\left(\frac{dX}{dt}\right)_{Carbonator} = k_s\, \phi\, X_{ave}\, \left(\overline{\nu_{CO2} - \nu_{CO2eq}}\right) \quad (3)$$

Here, $dX/dt_{Carbonator}$ (s^{-1}) is the reaction rate of the CaO particles in the carbonator, k_s is the reaction rate constant of the sorbent (s^{-1}), ν_{CO2} denotes the volume fractions of CO_2 in the carbonator. The parameter ϕ is a gas–solid contacting factor that accounts for physical limitations to carbonation relative to the intrinsic reaction rate (k_s), which is typically measured in the absence of external mass-transfer resistances (Rodriguez et al., 2011). The intrinsic rate k_s is determined by thermogravimetric (TG) analysis under conditions designed to minimize external diffusion effects, such as small sample masses and high gas velocities around the sample holder. The effective parameter $k_s\phi$ is obtained by fitting pilot-plant data to Equation 7, and ϕ is then calculated as the ratio between $k_s\phi$ and the intrinsic k_s measured in TG experiments. Finally, X_{ave} refers to the maximum CO_2 carrying capacity of the sorbent. This is a key feature in calcium looping systems, where the carrying capacity of individual particles circulating in the system decreases with the number of carbonation- calcination cycles (Grasa and Abanades, 2006). During the tests reported in this work, the pilot was operated with a wide range of CO_2 carrying capacities (0.15–0.36).

Using the approach indicated above, the mass balance equation for CO_2 removal from the gas phase and its capture by CaO particles in the carbonator bed can now be formulated as:

$$E_{Carb} = n_{Ca}\, f_a\, X_{ave}\, k_s\, \phi\, \left(\overline{\nu_{CO2} - \nu_{CO2eq}}\right) / F_{CO2,in} \quad (7)$$

In this equation, n_{Ca} represents the total calcium inventory in the carbonator, f_a is the fraction of active solids that have not yet reached X_{ave}, and F_{CO2} denotes the molar flow of CO_2 entering the reactor. These variables collectively define a term known as the active space time ($\tau_{active} = n_{Ca}\, f_a\, X_{ave}$ / $F_{CO2,\ in}$) (Charitos et al., 2011). The parameter $k_s\phi$ is determined as a fitting factor and found to be 0.36 s^{-1} for all the date reported in this work. This value compares favourably with previous

data obtained under conditions of oxy-combustion of coal in the carbonator.

Fig. 4 includes the values obtained with Eq. (7) (shown as solid and dotted lines) in two extreme cases that cover the wide range of inlet CO_2 concentration ($\nu_{CO2,in}$) tested during these experimental campaigns. Despite uncertainties linked to the estimation of certain variables in Eq. (7), the majority of the experimental data align well with the trends predicted by the model. This behavior is consistent with findings from previous studies where the calciner operated using coal as fuel. As can be seen, high CO_2 capture efficiencies, well above 0.95, are achieved during experiments where τ_{active} reaches a value higher than 75 s^{-1}. An extreme example of operation of a CFB-CaL system with high values of τ_{active} has been recently reported (Arias et al., 2024) to illustrate the technical viability of the carbonator of the La Pereda CFB-CaL pilot to achieve capture efficiencies over 99%. This was accomplished by operating the CaL pilot with large make up flows of limestone to reach X_{ave} close to 0.3 which resulted into values of τ_{active} values above 100 s^{-1}.

As noted above, in addition to steady state campaigns validating the adequate performance of the carbonator when using biomass as fuel in the oxy-fired calciner in standard conditions in the calcium looping system, the pilot was forced to operate under extreme combustion conditions in the calciner, targeting the generation of a CO_2-rich off gas from the calciner with low oxygen content (towards <2%v O_2). As an example, Fig. 5 plots the composition of O_2, CO, NO_x and unburnt hydrocarbons ($C_xH_yO_z$-estimated as the sum of CH_4, C_2H_6, C_2H_4, C_3H_8, C_6H_{14} and CHOH measured using the FTIR analyser) in the rich-CO_2 flue gas during an experimental period with low excess of oxygen, λ=1.04. The excess of oxygen (λ) is defined as the oxygen-to-fuel ratio relatively to the stoichiometric ratio. As can be observed, there are intense fluctuations in oxygen composition at the outlet of the calciner under such combustion conditions. Since the frequencies and amplitudes of such fluctuation coincide with those of other combustion species, these can be attributed to the temporal variations in the biomass flow rate actually entering the bed of the calciner. The presence (or lack of) of small batches of recently entered biomass pellets, that should volatilise at a high rate when entering the bed of solids in the calciner, would promote fluctuations in the instant excess oxygen in the calciner and hence the combustion conditions, especially when operating close to the stoichiometric conditions. Such phenomena are probably highly dependent on particular features of the solid feeding system of the pilot, the

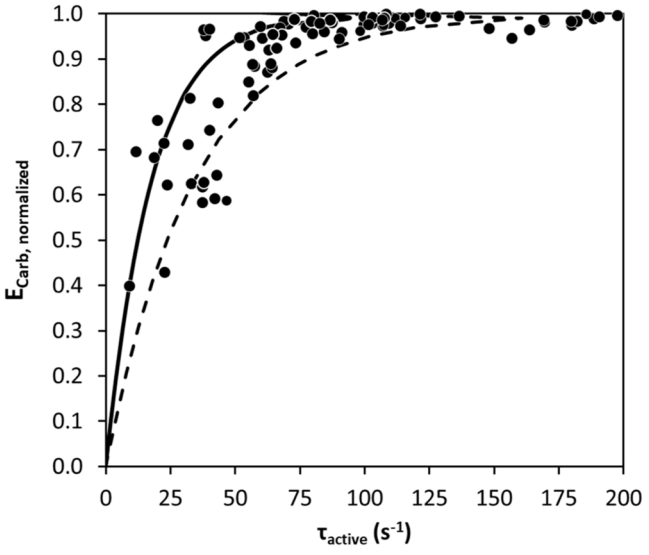

Fig. 4. Normalized CO_2 capture efficiency ($E_{carb,norm}=E_{carb}/E_{carb,eq}$) as a function of active space time, $\tau_{active} = n_{Ca}\ f_a\ X_{ave}\ /\ F_{CO2,\ in}$ Lines have been calculated using Eq. (3) with the following average values: T_{carb}=655 °C, $k_s\varphi$=0.36 s^{-1}, ν_{CO2in}=0.08 (solid line) and ν_{CO2in}=0.15 (dashed line)).

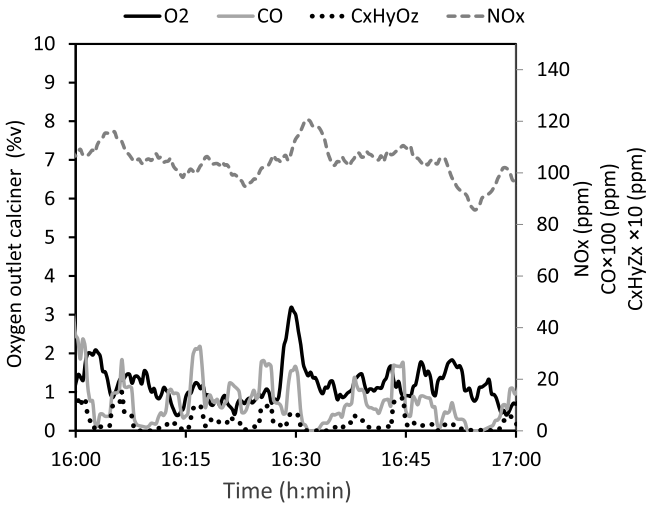

Fig. 5. Example of an experimental period operating the calciner with a low excess of oxygen during biomass combustion (average temperature in the calciner: 890 °C, outlet gas velocity in the calciner: 4.5 m/s, inventory of solids in the calciner: 180 kg/m^2).

geometry of the calciner bottom region, and the complex fluid-dynamics in such turbulent bed of solids (Ylatalo et al., 2012; Ylätalo et al., 2013; Ylätalo et al., 2014). In large scale systems, the buffer effect of much larger inventory of solids in the bottom region of the oxy-fired calciner and the proper fuel distribution along the cross-section area should help to maintain more stable conditions at the outlet of the reactor, although fuel and solid mixing phenomena is also a very important 3D modelling objective in large scale CFB combustors (Ylatalo et al., 2012; Ylätalo et al., 2013; Ylätalo et al., 2014). Despite the fluctuation observed, the results reported here should be useful to tune such 3D reactor models in future modelling efforts within the CaLby2030 project (Calby2030, 2022). As can be seen in the example of Fig. 5, when the average oxygen concentration at the outlet of the calciner is around 1.5%v, the CO emissions remain relatively low, averaging approximately 1100 ppm_v, with a few peaks below 3000 ppm_v. For unburnt hydrocarbons ($C_xH_yO_z$), average emissions are around 35 ppm, with peaks below 500 ppm_v. NO_x emissions during this period average 100 ppm_v. During standard oxy-fuel conditions such as those depicted in Fig. 3 (with oxygen concentrations at the outlet of the calciner around 4.5–5.0%v), no CO and $C_xH_yO_z$ emissions are detected, while NO_x emissions are measured at approximately 120 ppm_v.

Fig. 6 shows an example of results where the excess of oxygen in the calciner is eventually forced to values of λ<1 in the calciner, under which no oxygen should be expected at the exit of the calciner. To observe the potential impact of such conditions on the carbonator side, the graph in the left of Fig. 6 shows the inventory and temperature in both the carbonator and calciner. A flue gas with a CO_2 concentration of 13.6%v was fed into the carbonator. During the whole period, a high CO_2 capture efficiency (>0.95) was measured, consistent with a high value of τ_{active} =65 s, as discussed around Fig. 4. At the beginning of the test (before 11:40), the oxy-combustion in the calciner was carried out with a relatively high excess of oxygen (λ=1.65). Under these conditions (i.e. with an exit oxygen concentration around 6% in the rich-CO_2 gas leaving the calciner), no CO or $C_xH_yO_z$ are detected and the concentration of NO_x remained around 120 ppm. From this point, the excess of oxygen was reduced in three steps (λ<0.96, 0.88, 0.85), by progressively reducing the oxygen feeding rate and increasing the biomass feeding rate to the calciner. For an excess of oxygen slightly below the stoichiometric conditions (λ=0.96), there is an increase of the CO and $C_xH_yO_z$ emissions up to values around 8600 ppm and 760 ppm, respectively. In addition, an important reduction is observed on NO_x emissions, that drop until a value around 35 ppm, consistent with the

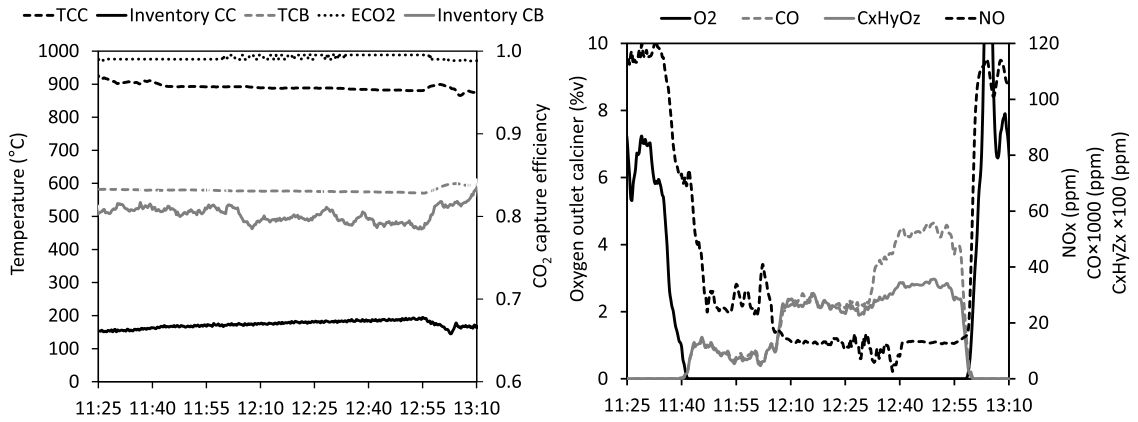

Fig. 6. Example of an experimental period operating the calciner under stoichiometric combustion conditions. Left: main operation conditions in the carbonator and calciner; right: composition of the rich-CO_2 flue gas leaving the calciner.

reducing conditions that must be present towards the top part of the calciner under the lower availability of oxygen (Duan et al., 2011; Stanger et al., 2015). A further decrease of the excess of oxygen, translates into drastic increases in CO and $C_xH_yO_z$ which can reach values up to values of 53,000 ppm and 3400 ppm, respectively, for a defect of oxygen of 0.85.

A comprehensive investigation into the influence of combustion conditions on the emission profiles of these gases lies beyond the scope of the present study. Such an analysis would necessitate application of advanced three-dimensional (3D) computational models capable of resolving localized phenomena (i.e. gas–solid interactions, spatial variations in the oxygen-to-fuel ratio) that are relatively well quantified in state-of-the-art models of CFB combustion power plants (Adamczyk et al., 2014; Gu et al., 2019; Kanellis et al., 2023; Ylätalo et al., 2013). Nonetheless, Fig. 7 provides a first plot of the trends observed during the experimental campaigns carried out using the excess of oxygen λ as parameter with each point representing a period of 30–200 min of stable conditions as those represented in Fig. 6.

For clarity, the emissions of unburnt hydrocarbons (CxHyOz) are not represented in Fig. 7 because they follow similar trend that the emissions of CO. Solid lines represent the experimentally observed trends, while the dashed line indicates the theoretical oxygen concentration in the CO_2-rich flue gas exiting the calciner, calculated under the assumption of

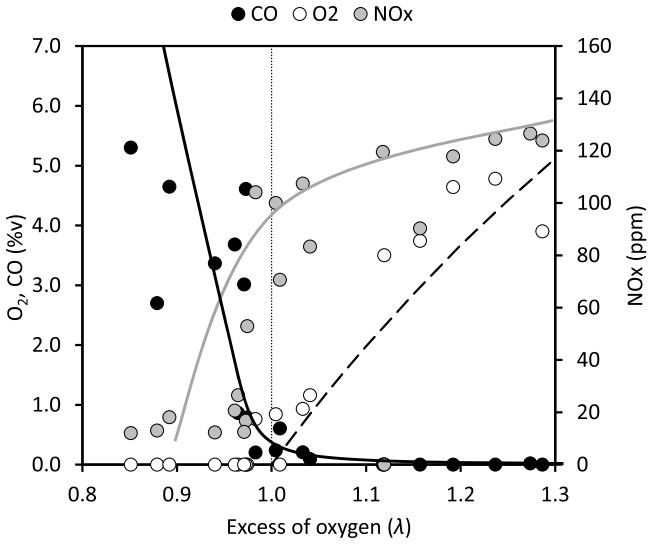

Fig. 7. Effect of excess of oxygen (λ) on CO and NOx emissions during biomass oxy-fuel combustion in the calciner (dots-experimental values; lines-experimental observed trends).

an average inlet oxygen concentration of 30%$_v$. As discussed above, the oxy-fired calciner can be operated under close to stoichiometric conditions without producing noticeable emissions of CO and $C_xH_yO_z$ and maintaining the performance of the CO_2 carbonator. However, a sharp increase on the emissions of CO (and other fuel gases) is observed as the oxygen excess is reduced below the stoichiometric conditions. On the other hand, the reducing conditions can greatly minimize the NO_x emissions, with values even below 20 ppm$_v$, compared with the standard range of between 120–130 when O_2 at the exit of the calciner is >5%$_v$. These results open the door to consider λ as a new key target for optimization in attempts to reduce the cost of the overall CCU/S system where the CaL system must be integrated. For example, as discussed above, the use of biomass as fuel in the oxy-fired calciner represent an opportunity to produce carbon-neutral synthetic products from CO_2 captured and released in the CO_2-rich gas raw stream leaving the calciner. Most of the routes to produce such synthetic products are based on catalysts which are negatively affected by the presence of oxygen and other impurities in the feed gas streams (Götz et al., 2016) but are not affected (or even benefit) by the presence of CO.

However, an excessive reduction in oxygen excess may lead to incomplete combustion of the solid fuel within the calciner, resulting in the carryover of unburned carbon in solid form to the carbonator and a decrease in fuel utilization in the calciner. Moreover, this would lead to an additional increase heat release in the carbonator, both from the combustion of the transported fuel and from the exothermic carbonation of the additional CO_2 produced. Since combustion within the carbonator is undesirable—given its primary function is CO_2 capture—this shift in heat distribution may negatively impact the whole CaL system. The interplay between these opposing effects highlights a trade-off that should be addressed through more comprehensive modelling efforts. Such analyses could be supported and validated using the experimental data and trends reported in this work.

4. Conclusions

This study presents recent advancements in calcium looping technology, demonstrated through experimental campaigns conducted at the upgraded 1.7 MW_{th} La Pereda pilot facility. These efforts aim to generate Technology Readiness Level 6 (TRL6) data relevant to biomass-fired applications. The pilot plant has been retrofitted to enable biomass combustion within the oxy-fired circulating fluidized bed calciner, allowing a series of CO_2 capture experiments to be performed. The trials confirmed the feasibility of operation under oxy-combustion conditions with low residual O_2 concentrations at the calciner outlet—an outcome that may support CO_2 purification by lowering NO_x emissions (up to values below 20 ppmv) and reducing or avoiding the presence of oxygen. However, the operation under sub-stoichiometric conditions (λ<1)

may lead to CO and unburnt hydrocarbons levels that may not be acceptable if the fate of the CO_2 is transport for permanent storage. These results contribute to the broader objective of validating calcium looping as a viable pathway for decarbonizing carbon-intensive industries and advancing the technology toward large-scale implementation.

CRediT authorship contribution statement

Borja Arias: Writing – review & editing, Writing – original draft, Methodology, Investigation, Formal analysis, Conceptualization. **Alberto Méndez:** Methodology, Formal analysis. **Yolanda Álvarez Criado:** Writing – original draft, Methodology. **Paula Marqués:** Formal analysis. **Roberto García:** Formal analysis. **Javier Camús:** Formal analysis. **Igor Finca:** Investigation. **Martin Haaf:** Writing – review & editing. **J.Carlos Abanades:** Writing – review & editing, Writing – original draft, Supervision, Conceptualization.

Declaration of competing interest

The authors declare that they have no known competing financial interests or personal relationships that could have appeared to influence the work reported in this paper.

Acknowledgements

The authors acknowledge the financial support from the CaLby2030 project, which has received funding from the European Union's Horizon Europe research and innovation program under grant agreement No. 101075416. We also wish to thank the support during these experiments and the material characterization works from M. Alonso, M.E. Diego, L. Suárez, F. Fuentes of CSIC, E. de la Llera and M. Lorenzo of HUNOSA, and S. Summaria and K. Vanska from SFW.

References

Abanades, J.C., Alonso, M., Rodríguez, N., González, B., Grasa, G., Murillo, R., 2009. Capturing CO_2 from combustion flue gases with a carbonation calcination loop. Experimental results and process development. Energ. Proced. 1 (1), 1147–1154. https://doi.org/10.1016/j.egypro.2009.01.151.

Adamczyk, W.P., Kozołub, P., Węcel, G., Klimanek, A., Białecki, R.A., Czakiert, T., 2014. Modeling oxy-fuel combustion in a 3D circulating fluidized bed using the hybrid Euler–Lagrange approach. Appl. Therm. Eng. 71 (1), 266–275. https://doi.org/10.1016/J.APPLTHERMALENG.2014.06.063.

Alonso, M., Diego, M.E., Pérez, C., Chamberlain, J.R., Abanades, J.C., 2014. Biomass combustion with in situ CO_2 capture by CaO in a 300kWth circulating fluidized bed facility. Int. J. Greenh. Gas Contr. 29, 142–152. https://doi.org/10.1016/j.ijggc.2014.08.002.

Alonso, M., Rodríguez, N., Grasa, G., Abanades, J.C., 2009. Modelling of a fluidized bed carbonator reactor to capture CO_2 from a combustion flue gas. Chem. Eng. Sci. 64 (5), 883–891. https://doi.org/10.1016/J.CES.2008.10.044.

Arias, B., et al., 2013. Demonstration of steady state CO_2 capture in a 1.7 MW_{th} calcium looping pilot. Int. J. Greenh. Gas Contr. 18 (0), 237–245. https://doi.org/10.1016/j.ijggc.2013.07.014.

Arias, B., Alvarez Criado, Y., Méndez, A., Marqués, P., Finca, I., Abanades, J.C., 2024. Pilot testing of calcium looping at TRL7 with CO_2 capture efficiencies toward 99%. Energy & Fuels 38 (15), 14757–14764. https://doi.org/10.1021/acs.energyfuels.4c02472.

Arias, B., Diego, M.E., Méndez, A., Alonso, M., Abanades, J.C., 2018. Calcium looping performance under extreme oxy-fuel combustion conditions in the calciner. Fuel 222, 711–717. https://doi.org/10.1016/j.fuel.2018.02.163.

Baker, E.H., 1962. The calcium oxide-carbon dioxide system in the pressure range 1-300 atmospheres. J. Chem. Soc. (0), 464–470. https://doi.org/10.1039/JR9620000464.

Calby2030, "Calcium looping to capture CO2 from industrial processes by 2030. www.calby2030.eu," 2022.

Chang, M.H., et al., 2013. Design and experimental investigation of calcium looping process for 3-kW_{th} and 1.9-MW_{th} facilities. Chem. Eng. Technol. 36 (9), 1525–1532. https://doi.org/10.1002/ceat.201300081.

Charitos, A., et al., 2011. Experimental validation of the calcium looping CO_2 capture process with two circulating fluidized bed carbonator reactors. Ind. Eng. Chem. Res. 50 (16), 9685–9695. https://doi.org/10.1021/ie200579f.

Charitos, A., et al., Jul. 2011. Experimental validation of the calcium looping CO_2 capture process with two circulating fluidized bed carbonator reactors. Ind. Eng. Chem. Res. 50 (16), 9685–9695. https://doi.org/10.1021/ie200579f.

Diego, M.E., et al., 2014. Calcium looping with enhanced sorbent performance: experimental testing in A large pilot plant. Energ. Proced. 63 (0), 2060–2069. https://doi.org/10.1016/j.egypro.2014.11.222.

Diego, M.E., et al., 2016. Experimental testing of a sorbent reactivation process in La Pereda 1.7 MW_{th} calcium looping pilot plant. Int. J. Greenh. Gas Contr. 50, 14–22. https://doi.org/10.1016/j.ijggc.2016.04.008.

Diego, M.E., Alonso, M., 2016. Operational feasibility of biomass combustion with in situ CO2 capture by CaO during 360h in a 300kW_{th} calcium looping facility. Fuel 181, 325–329. https://doi.org/10.1016/j.fuel.2016.04.128.

Diego, M.E., Arias, B., Apr. 2020. Impact of load changes on the carbonator reactor of a 1.7 MW_{th} calcium looping pilot plant. Fuel Process. Technol. 200, 106307. https://doi.org/10.1016/J.FUPROC.2019.106307.

Dieter, H., Hawthorne, C., Zieba, M., Scheffknecht, G., 2013. Progress in calcium looping post combustion CO_2 capture: successful pilot scale demonstration. Energ. Proced. 37 (0), 48–56. https://doi.org/10.1016/j.egypro.2013.05.084.

Duan, L., Zhao, C., Zhou, W., Qu, C., Chen, X., 2011. Effects of operation parameters on NO emission in an oxy-fired CFB combustor. Fuel Process. Technol. 92 (3), 379–384. https://doi.org/10.1016/J.FUPROC.2010.09.031.

García-Labiano, F., Abad, A., de Diego, L.F., Gayán, P., Adánez, J., 2002. Calcination of calcium-based sorbents at pressure in a broad range of CO_2 concentrations. Chem. Eng. Sci. 57 (13), 2381–2393. https://doi.org/10.1016/S0009-2509(02)00137-9.

Götz, M., et al., 2016. Renewable Power-to-gas: a technological and economic review. Renew. Energy 85, 1371–1390. https://doi.org/10.1016/j.renene.2015.07.066.

Grasa, G.S., Abanades, J.C., 2006. CO_2 capture capacity of CaO in long series of carbonation/calcination cycles. Ind. Eng. Chem. Res. 45 (26), 8846–8851 [Online]. Available: http://www.scopus.com/inward/record.url?eid=2-s2.0-33846228686&partnerID=40&md5=78ae62f2cdf2f4cbac890b93377d16ad.

Greco-Coppi, M., Ströhle, J., Epple, B., 2025. A carbonator model for CO_2 capture based on results from pilot tests. Part II: deactivation and reaction model. Chem. Eng. J. 508, 159041. https://doi.org/10.1016/j.cej.2024.159041.

Gu, J., Zhong, W., Yu, A., 2019. Three-dimensional simulation of oxy-fuel combustion in a circulating fluidized bed. Powder Technol. 351, 16–27. https://doi.org/10.1016/J.POWTEC.2019.04.008.

Haaf, M., Hilz, J., Peters, J., Unger, A., Ströhle, J., Epple, B., Jul. 2020. Operation of a 1 MW_{th} calcium looping pilot plant firing waste-derived fuels in the calciner. Powder Technol. 372, 267–274. https://doi.org/10.1016/J.POWTEC.2020.05.074.

Haaf, M., Peters, J., Hilz, J., Unger, A., Ströhle, J., Epple, B., 2020. Combustion of solid recovered fuels within the calcium looping process – Experimental demonstration at 1 MW_{th} scale. Exp. Therm. Fluid Sci. 113. https://doi.org/10.1016/j.expthermflusci.2019.110023.

Hanak, D.P., Anthony, E.J., Manovic, V., 2015. A review of developments in pilot-plant testing and modelling of calcium looping process for CO_2 capture from power generation systems. Energy Environ. Sci. 8 (8), 2199–2249. https://doi.org/10.1039/C5EE01228G.

Hills, A.W.D., 1968. Equilibrium decomposition pressure of calcium carbonate between 700 and 900°C. Bull. Inst. Min. Metall. 76D, 241–246.

Hilz, J., Helbig, M., Haaf, M., Daikeler, A., Ströhle, J., Epple, B., 2017. Long-term pilot testing of the carbonate looping process in 1 MW_{th} scale. Fuel 210, 892–899. https://doi.org/10.1016/j.fuel.2017.08.105.

IEAGHG, "Impact of CO2 impurity on CO2 compression, liquefaction and transportation," 2016.

IPCC, 2005. Special report on carbon dioxide capture and storage. In: Metz, B., Davidson, O., Coninck, H.C., Loos, M., Meyer, L.J. (Eds.), Prep. By Work. Gr. III Intergov. Panel Clim. Chang. Cambridge Univ. Press, Cambridge, United Kingdom/New York, NY, USA, p. 442 (available. www.ipcc.ch.

Kanellis, G., et al., Aug. 2023. CFD modelling of an indirectly heated calciner reactor, utilized for CO2 capture, in an eulerian framework. Fuel 346, 128251. https://doi.org/10.1016/J.FUEL.2023.128251.

Koohestanian, E., Shahraki, F., 2021. Review on principles, recent progress, and future challenges for oxy-fuel combustion CO_2 capture using compression and purification unit. J. Environ. Chem. Eng. 9 (4), 105777. https://doi.org/10.1016/J.JECE.2021.105777.

Lasheras, A., Ströhle, J., Galloy, A., Epple, B., 2011. Carbonate looping process simulation using a 1D fluidized bed model for the carbonator. Int. J. Greenh. Gas Contr. 5 (4), 686–693 [Online]. Available: http://www.scopus.com/inward/record.url?eid=2-s2.0-80051475609&partnerID=40&md5=cc6cda2ae8336dfcfd4b082206646d1e.

Magli, F., Spinelli, M., Fantini, M., Romano, M.C., Gatti, M., 2022. Techno-economic optimization and off-design analysis of CO_2 purification units for cement plants with oxyfuel-based CO_2 capture. Int. J. Greenh. Gas Contr. 115, 103591. https://doi.org/10.1016/J.IJGGC.2022.103591.

Martínez, I., et al., 2016. Review and research needs of Ca-looping systems modelling for post-combustion CO2 capture applications. Int. J. Greenh. Gas Contr. 50, 271–304. https://doi.org/10.1016/j.ijggc.2016.04.002.

Moreno, J., Hornberger, M., Schmid, M., Scheffknecht, G., 2021. Oxy-fuel combustion of hard coal, wheat straw, and solid recovered fuel in a 200 kw_{th} calcium looping CFB calciner. Energies 14 (8). https://doi.org/10.3390/en14082162.

Okeke, I.J., Ghantous, T., and Adams, T.A., "Design strategies for oxy-combustion power plant captured CO2 purification," vol. 18, no. 1, pp. 135–154, 2023, doi: 10.1515/cppm-2021-0041.

Perejón, A., Romeo, L.M., Lara, Y., Lisbona, P., Martínez, A., Valverde, J.M., 2016. The calcium-looping technology for CO_2 capture: on the important roles of energy integration and sorbent behavior. Appl. Energy 162 (Supplement C), 787–807. https://doi.org/10.1016/j.apenergy.2015.10.121.

Porter, R.T.J., Fairweather, M., Pourkashanian, M., Woolley, R.M., 2015. The range and level of impurities in CO_2 streams from different carbon capture sources. Int. J. Greenh. Gas Contr. 36, 161–174. https://doi.org/10.1016/j.ijggc.2015.02.016.

Rodriguez, N., Alonso, M., Abanades, J., 2011. Experimental investigation of a circulating fluidized-bed reactor to capture CO_2 with CaO. AIChE J 57 (5), 1356–1366. https://doi.org/10.1002/aic.12337.

Romano, M.C., 2012. Modeling the carbonator of a Ca-looping process for CO_2 capture from power plant flue gas. Chem. Eng. Sci. 69 (1), 257–269. https://doi.org/10.1016/j.ces.2011.10.041.

Sala, L., Zaryab, S.A., Chiesa, P., Martelli, E., 2024. Comparison and optimization of CO_2 purification units for CCS applications. Int. J. Greenh. Gas Contr. 136, 104193. https://doi.org/10.1016/J.IJGGC.2024.104193.

Shimizu, T., Hirama, T., Hosoda, H., Kitano, K., Inagaki, M., Tejima, K., 1999. A twin fluid-bed reactor for removal of CO_2 from combustion processes. Chem. Eng. Res. Des. 77 (1), 62–68. https://doi.org/10.1205/026387699525882.

Sonke, J., Bos, W.M., Paterson, S.J., 2022. Materials challenges with CO_2 transport and injection for carbon capture and storage. Int. J. Greenh. Gas Contr. 114, 103601. https://doi.org/10.1016/J.IJGGC.2022.103601.

Stanger, R., et al., 2015. Oxyfuel combustion for CO_2 capture in power plants. Int. J. Greenh. Gas Contr. 40, 55–125. https://doi.org/10.1016/j.ijggc.2015.06.010.

Ströhle, J., Junk, M., Kremer, J., Galloy, A., Epple, B., 2014. Carbonate looping experiments in a 1 MW_{th} pilot plant and model validation. Fuel 127, 13–22 [Online]. Available: http://www.scopus.com/inward/record.url?eid=2-s2.0-84897492477&partnerID=40&md5=d3a34c67550b8d785276a75cf42bd492.

Ströhle, J., Lasheras, A., Galloy, A., Epple, B., 2009. Simulation of the carbonate looping process for post-combustion CO_2 capture from a coal-fired power plant. Chem. Eng. Technol. 32 (3), 435–442. https://doi.org/10.1002/ceat.200800569.

Tan, Y., Liu, W., Zhang, X., Wei, W., Wang, S., 2024. Conventional and optimized testing facilities of calcium looping process for CO_2 capture: a systematic review. Fuel 358, 130337. https://doi.org/10.1016/J.FUEL.2023.130337.

Ylätalo, J., Parkkinen, J., Ritvanen, J., Tynjälä, T., Hyppänen, T., 2013. Modeling of the oxy-combustion calciner in the post-combustion calcium looping process. Fuel 113 (Supplement C), 770–779. https://doi.org/10.1016/j.fuel.2012.11.041.

Ylatalo, J., Ritvanen, J., Arias, B., Tynjala, T., Hyppanen, T., 2012. 1-Dimensional modelling and simulation of the calcium looping process. Int. J. Greenh. Gas Contr. 9, 130–135. https://doi.org/10.1016/j.ijggc.2012.03.008.

Ylätalo, J., Ritvanen, J., Tynjälä, T., Hyppänen, T., 2014. Model based scale-up study of the calcium looping process. Fuel 115, 329–337. https://doi.org/10.1016/j.fuel.2013.07.036.